

NACA TN 4402 9701



NATIONAL ADVISORY COMMITTEE FOR AERONAUTICS

TECHNICAL NOTE 4402

MEASUREMENTS OF AERODYNAMIC FORCES AND
MOMENTS AT SUBSONIC SPEEDS ON A SIMPLIFIED T-TAIL
OSCILLATING IN YAW ABOUT THE FIN MIDCHORD

By Sherman A. Clevenson and Sumner A. Leadbetter

Langley Aeronautical Laboratory
Langley Field, Va.



Washington
September 1958

AFMDC



0067190

NATIONAL ADVISORY COMMITTEE FOR AERONAUTICS

TECHNICAL NOTE 4402

MEASUREMENTS OF AERODYNAMIC FORCES AND
MOMENTS AT SUBSONIC SPEEDS ON A SIMPLIFIED T-TAIL
OSCILLATING IN YAW ABOUT THE FIN MIDCHORD

By Sherman A. Clevenson and Sumner A. Leadbetter

SUMMARY

Results are presented of some experimental measurements of aerodynamic forces and moments acting on a simplified T-tail configuration which is oscillating in yaw about an axis through the midchord of the vertical fin. Coefficients which define rolling moment of the horizontal stabilizer alone and rolling moment, yawing moment, and side force of the complete T-tail are shown. In the investigation the range of reduced-frequency parameter was from 0.09 to 0.56, the Mach number range was from 0.13 to 0.50, and the Reynolds number range was from 0.90×10^6 to 8.21×10^6 .

Coefficients for the steady case (reduced-frequency parameter of zero) were calculated for the forces and moments and good agreement was indicated for all except the horizontal-stabilizer rolling-moment coefficient which was found to be of greater magnitude than was indicated by the steady-state results. Some further comparisons were made of the side-force and yawing moment on the complete T-tail with results obtained from a previous investigation for a configuration consisting of a tip tank mounted on a plan form similar to the T-tail fin alone and were found to be compatible.

INTRODUCTION

The use of T-tail configurations on some present-day aircraft has introduced the problem of determining values to be assigned the aerodynamic forces and moments associated with the yawing oscillations of the components of the configuration. Some measurements of the aerodynamic forces and pressures acting on a T-tail configuration have been made for the steady-flow condition (for example, refs. 1 and 2), but there is a paucity of data, both analytical and experimental, for the unsteady-flow condition. As a result of the scarcity of information,

the validity of a flutter analysis for a T-tail configuration may be subject to question. In particular, little is known about the magnitude and phase angle of the oscillatory rolling moment acting on the horizontal stabilizer. In order to further the knowledge of the unsteady aerodynamic forces on T-tails, a limited investigation has been made of the aerodynamic forces and moments associated with the yawing oscillations of a simplified T-tail which consists of a low-aspect-ratio fin having a horizontal stabilizer at its tip.

The T-tail configuration was oscillated in yaw about an axis along the center line of the fin. Of primary interest was the rolling moment on the horizontal stabilizer due to the angular (yawing) motion of the fin. Of secondary importance were the overall side forces, the yawing moments, and the rolling moments on the entire T-tail.

The aerodynamic coefficients are presented for a range of reduced-frequency parameter from 0.09 to 0.56, of Mach number from 0.13 to 0.50, and of Reynolds number from 0.90×10^6 to 8.21×10^6 . These measurements were made in the Langley 2-foot transonic flutter tunnel.

SYMBOLS

| | |
|-----------------|---|
| c | chord of fin, ft |
| F_Y | oscillating side force acting on T-tail, positive in direction of leading edge of fin moving to right, $\pi q S \psi C_{Y,\psi}$ |
| g_t | damping coefficient of T-tail in airstream |
| g_{vac} | damping coefficient of T-tail in a near vacuum |
| I_e | effective moment of inertia of oscillating system, ft-lb-sec ² |
| $i = \sqrt{-1}$ | |
| K_s | effective spring constant of oscillating system, ft-lb/radian |
| k | reduced-frequency parameter, $\omega c / 2V$ |
| M_ψ | oscillating yawing moment about root midchord of fin, positive in direction of leading edge of fin moving to right, $\pi q S (c/2) \psi C_{n,\psi}$ |

| | |
|---|---|
| M_ϕ | oscillating rolling moment about an axis 6 inches inboard of root of fin, positive in direction of fin tip moving to right, $\pi q S(c/2) \psi C_{l,\psi}$ |
| $M_{\phi'}$ | horizontal-stabilizer oscillating rolling moment about junction of fin and of horizontal stabilizer, positive in direction of right tip of horizontal stabilizer moving down, $\pi q S(c/2) \psi C_{l',\psi}$ |
| q | dynamic pressure, lb/sq ft |
| S | area of fin, sq ft |
| t | time, sec |
| V | velocity of airstream, ft/sec |
| ω | circular frequency of oscillation of T-tail, radians/sec |
| ω_{vac} | circular frequency of oscillation of T-tail in a near vacuum, radians/sec |
| ψ | angle of yaw at midspan station of fin as a function of time, positive for leading edge moving to the right, $ \psi e^{i\omega t}$, radians |
| $(C_Y, \psi)_r, (C_Y, \psi)_i$, and so forth | real and imaginary components of complex coefficients due to yaw; for example, for side force, $C_{Y,\psi} = (C_{Y,\psi})_r + i(C_{Y,\psi})_i$ |
| $ C_{Y,\psi} $ | magnitude of side-force coefficient due to yaw, $\sqrt{[(C_{Y,\psi})_r]^2 + [(C_{Y,\psi})_i]^2}$ |
| $ C_{n,\psi} $ | magnitude of yawing-moment coefficient due to yaw, $\sqrt{[(C_{n,\psi})_r]^2 + [(C_{n,\psi})_i]^2}$ |
| $ C_{l,\psi} $ | magnitude of total rolling-moment coefficient due to yaw, $\sqrt{[(C_{l,\psi})_r]^2 + [(C_{l,\psi})_i]^2}$ |
| $ C_{l',\psi} $ | magnitude of horizontal-stabilizer rolling-moment coefficient due to yaw, $\sqrt{[(C_{l',\psi})_r]^2 + [(C_{l',\psi})_i]^2}$ |

| | |
|------------------|--|
| $\phi_{Y,\psi}$ | phase angle between side force F_Y and displacement in yaw (positive when force vector leads displacement), $\tan^{-1} \frac{(C_Y, \psi)_i}{(C_Y, \psi)_r}$, deg |
| $\phi_{n,\psi}$ | phase angle between yawing moment M_ψ and displacement in yaw (positive when moment vector leads displacement), $\tan^{-1} \frac{(C_n, \psi)_i}{(C_n, \psi)_r}$, deg |
| $\phi_{l,\psi}$ | phase angle between total rolling moment M_ϕ and displacement in yaw (positive when moment vector leads displacement), $\tan^{-1} \frac{(C_l, \psi)_i}{(C_l, \psi)_r}$, deg |
| $\phi_{l',\psi}$ | phase angle between horizontal-stabilizer rolling moment $M_{\phi'}$ and displacement in yaw (positive when moment vector leads displacement), $\tan^{-1} \frac{(C_{l'}, \psi)_i}{(C_{l'}, \psi)_r}$, deg |

APPARATUS AND METHOD

The apparatus, techniques of measurement, and methods of data reduction employed in the present investigation are similar to the equipment and procedures which have been developed and used previously in related studies (for example, refs. 3 and 4). This section gives details of the equipment and methods pertinent to the present problem.

Tunnel

The Langley 2-foot transonic flutter tunnel with the slots replaced with solid walls was used for the present investigation. This tunnel is of the closed-throat single-return type. The testing medium employed for these measurements was either air or Freon-12 at atmospheric pressure.

Model

The T-tail model consisted of a 12-inch span, 12-inch-chord vertical fin with a 12-inch-span 12-inch-chord horizontal stabilizer mounted at

the fin tip. (See fig. 1.) Fabricated construction was used for both the fin and stabilizer. The fin consisted of a steel box spar located at the axis of rotation, carrying four evenly spaced ribs to which plywood skin was attached in order to form an NACA 65A010 airfoil section. The horizontal stabilizer was constructed of three balsa ribs covered with balsa planking to form an NACA 65A010 airfoil. Steel stiffeners were fastened around the center part of the stabilizer where it was connected to the strain-gage balances at the tip of the vertical fin. A silk fairing, extending $1\frac{1}{2}$ inches on each side of the center line of the stabilizer, was placed at the junction of the vertical fin and the horizontal stabilizer to prevent air flow between them.

The fin-stabilizer combination was mounted as a cantilever in an oscillator mechanism which permitted the T-tail to oscillate in yaw about an axis along the midchord of the fin. (See fig. 2.) The combination was mass-balanced about the axis of oscillation in such a manner that there was small side-force reaction when the model was oscillated in a near vacuum.

The vertical fin was designed to have high natural frequencies in order to reduce the amount of correction to the measured forces due to elastic deformations and to bending inertia loads. The first natural cantilever bending frequency of the fin alone was 130 cycles per second. The natural rolling frequency of the horizontal stabilizer on the strain-gage balance was 131 cycles per second and the natural bending frequency of the fin-stabilizer combination was 68 cycles per second. During the tests the frequency of yawing oscillation of the system varied from 18 to 14.1 cycles per second.

Oscillator Mechanism

The oscillator mechanism may be considered as a simple, torsional, vibratory system consisting of a torsion spring fixed at one end and attached to a bearing-supported hollow steel tube to which the model and base plate are clamped. (See fig. 2.) The mechanism was oscillated in torsion at the natural frequency of the simple spring-inertia system by applying a harmonically varying torque through shaker coils attached to the steel tube. In a near vacuum, this natural frequency was approximately 18 cycles per second.

The bearings were contained in housings which were carried on strain-gage dynamometers from which the side force and rolling moment could be determined. These dynamometers were of the force-displacement type and had a full-scale deflection of 0.0015 inch. The vertical reactions at the fixed end of the torsion spring were negligible because of the

flexibility of the torque rod and the small deformations experienced by the strain-gage dynamometers.

The electromagnetic shakers, which furnished torque to the system, consisted of stationary coils supplying a steady magnetic field and moving coils which were attached to the steel tube. The moving coils were driven by a variable-frequency oscillator. These moving coils were alined so that the direction of the applied forces was perpendicular to the direction of the side force. Provision was made for interrupting the power to the moving coils in order to obtain a power-off decaying oscillation. During the tests, the amplitude of oscillation was $\pm 2.8^\circ$.

Instrumentation

The instrumentation was designed to provide continuous signals that were proportional to the side force acting on the fin, the rolling moment of the complete T-tail, the rolling moment of the stabilizer about the tip of the fin, and the angular position in yaw of the fin. Figure 3 indicates the axes and the positive directions of the forces and moments. The side-force and total rolling-moment signals were obtained from the appropriate summation of the electrical outputs of the strain-gage dynamometers. (See fig. 2.) The stabilizer was mounted on miniature strain-gage dynamometers sensitive only to the rolling moment of the stabilizer. The electrical signals were filtered to eliminate noise and higher harmonics and then amplified, and their magnitudes were measured by using a vacuum-tube voltmeter.

The angular position was determined from the output of torsion strain gages mounted on the torque rod. This signal was recorded on a recording oscillograph both during the forced oscillation of the model and during the decay of the oscillation.

Phase measurements were made electronically of the signals representing resultant vectors of the forces and read on a meter calibrated in degrees. This electronic measurement was made by determining the time lapse between a given point on the side-force (or moment) signal and a corresponding point on the position signal while the T-tail configuration was oscillated at a constant frequency.

Calibration

The angular position of the model was dynamically calibrated in still air with the signal from the torsion strain gages by a photographic technique. Time exposures were taken of a fine chordwise thread on the outer (upper) surface of the horizontal stabilizer for various amplitudes while the strain-gage output was recorded. The amplitude of oscillation of the model was obtained from the envelope position of the

thread on the outer surface of the stabilizer and correlated with the strain-gage signal. By using this calibration along with a calibration made with the T-tail configuration replaced by an equivalent moment of inertia and the thread placed on the root clamp, it was determined that, at the maximum frequency of oscillation (18 cycles per second), the tip angle of attack exceeded the root angle of attack of the fin by 6 percent.

The signals from the strain-gage dynamometers were calibrated in terms of pounds of force per unit of signal strength for the side force and in foot-pounds per unit of signal strength for the moments. For the side force and the total rolling moment, known loads were applied to the fin at given distances from the roll axis and the dynamometers were calibrated from the mechanics of the system, that is, by treating the model-trunnion system as a simply supported beam having overhang and having supports at the bearings. (See fig. 2.) The reaction forces and moments were then related to the respective signals. The vacuum-tube voltmeter was calibrated dynamically by using a low-frequency oscillator and a voltage divider. These dynamic calibrations were then related to forces by use of the open-circuit load calibration of the strain gages. The readings from the vacuum-tube voltmeter are believed to be within ± 3 percent of true signal. No correction was made to the measured rolling moment on the horizontal stabilizer. Although a rotation of the stabilizer about its axis or a bending deflection of the vertical fin would cause a rolling moment on the horizontal stabilizer, a calculation of this correction for the worst condition - namely, highest Mach number - was less than 1 percent of the measured moment. For the wind-off condition, the tare values amounted to only 3 percent of the maximum measured rolling moment.

The phase-measuring system was calibrated at various frequencies by using standard resistance-capacitance phase-shift circuits. Calibrations of the phasemeter indicated that the phase angle may be determined within $\pm 2^\circ$ of true value. In order to minimize errors in phase introduced in the electrical operations, a tare value of phase was obtained at each reading by applying simultaneously the angular-position signals through both channels of the electrical circuits.

Data Reduction

The total side forces as received from the dynamometers contain an aerodynamic component and an inertia component which arise from the bending deformation of the fin. In appendix A of reference 3 a correction factor is developed which, when multiplied by the measured side force, gives the actual applied side force due to yaw. For the present problem the value of this factor is 0.955. The phase angle $\phi_{Y,\psi}$ contained a component due to bending deformation that tended to increase

$\phi_{Y,\psi}$ by less than 0.1° . The total rolling moments due to the bending deflection of the fin were found to be negligible relative to the magnitude of the measured moment. Since the aerodynamic effects due to fin bending were within the accuracy of the measurement, no effort was made to adjust for these quantities.

The inphase yawing moment on the fin-stabilizer combination was determined from the change in resonant frequency due to air flowing over the model. Since the torsional damping was small, its effect on the frequency is neglected and the entire shift is attributed to the inphase moment. The yawing-moment coefficient in phase with the yawing angular displacement is given by

$$-(C_{n,\psi})_r = \frac{K_s}{\pi q S} \frac{c}{2} \left[\left(\frac{\omega}{\omega_{vac}} \right)^2 - 1 \right]$$

The derivation of this equation is treated in appendix A of reference 4. The dependency of $(C_{n,\psi})_r$ on the small difference of two quantities of approximately the same magnitude leads to considerable loss in accuracy and consequent scatter in the data.

The quadrature-moment coefficient for the fin-stabilizer combination was determined by operating on the time history of the yawing angular position obtained during the power-off decay of the oscillation. The moment coefficient in phase with the angular velocity is given by

$$-(C_{n,\psi})_i = \frac{I_e \omega^2}{\pi q S} \frac{c}{2} \left[g_t - \left(\frac{\omega_{vac}}{\omega} \right)^2 g_{vac} \right]$$

The derivation of this equation is treated in appendix B of reference 3.

The phase angle $\phi_{n,\psi}$ between the yawing moment of the T-tail and the yaw angle was obtained from the relationship

$$\phi_{n,\psi} = \tan^{-1} \frac{(C_{n,\psi})_i}{(C_{n,\psi})_r}$$

The rolling moments on the horizontal stabilizer were obtained from the outputs of the strain-gage balances, and the phase angles were determined from the phasemeter.

RESULTS AND DISCUSSION

The experimental results for the measured aerodynamic forces, moments, and phase angles for a T-tail configuration are given in table I. Also given in this table are the corresponding reduced-frequency parameters and dynamic pressures. In order to show trends and comparisons, the experimental values are plotted in figures 4 to 7.

Included in figures 4 to 7 are calculated results for the steady case ($k = 0$). These results have been obtained by application of the four-vortex lifting-line procedure of reference 2, modified to account for the presence of the tunnel wall. The yawing moment and side force for the complete T-tail are also compared with experimental results from reference 3 for a plan form very similar to the fin alone and for this plan form carrying a tip tank.

All the coefficients presented are normalized by dynamic pressure q , an area S , and the yawing angle ψ . The moments are also normalized to a reference chord $\frac{c}{2}$. The sign convention employed for the data presented is indicated in figure 3.

Horizontal-Stabilizer Rolling Moments

The horizontal-stabilizer rolling-moment coefficients $|C_{l'}|$ and phase angles $\phi_{l',\psi}$ are shown in figure 4. The phase angle represents the amount of lead or lag of this rolling moment with the yawing position. As may be seen in the upper portion of figure 4, the phase angle $\phi_{l',\psi}$ is slightly negative through the lower range of reduced-frequency parameter k investigated. This means that the rolling moment on the stabilizer slightly lags the position of the rudder in the lower range of k . In general, the phase angles increased with increasing k .

The magnitude of the horizontal-stabilizer rolling-moment coefficient is indicated in the lower portion of figure 4. It may be seen that, as k is increased, the horizontal-stabilizer rolling-moment coefficient decreases considerably. The conclusion may be drawn that reduced-frequency parameter has some effect on the rolling moment and its phase angle in the range of k investigated. Also, inasmuch as there is little information about the oscillatory rolling moments acting on horizontal tail surfaces, it is of interest to note the magnitude of these moment coefficients. Other work has indicated that the magnitude of this coefficient is quite small; that is, it might be negligible in a flutter analysis. For comparison, a value calculated for $k = 0$ by

use of the four-vortex lifting-line procedure of reference 2, modified to account for the presence of the tunnel wall, is included in figure 4. Also shown in this figure is a calculated value of the horizontal-stabilizer rolling moment from the results of reference 1. As can be seen, both of these calculated values are considerably below an extrapolation of the measured magnitudes.

Total Rolling Moment

The total rolling-moment coefficients $|C_{l,\psi}|$ and corresponding phase angles $\phi_{l,\psi}$ are given in figure 5. For comparison, a calculated point for $k = 0$ (calculation based on procedure of ref. 2) is also presented in this figure and good agreement is indicated. The total rolling-moment coefficient has the same form as the horizontal-stabilizer rolling-moment coefficient and the phase angle again refers to the yawing angle of the rudder. It may be seen that the phase angle increases somewhat (from -1° to 4°) over the range of k shown while the total rolling moment decreases slightly. Thus, it is seen that reduced-frequency parameter has small effect on the magnitude of the total-rolling-moment coefficients.

Total Yawing Moment

The total yawing-moment coefficients $|C_{n,\psi}|$ and phase angles $\phi_{n,\psi}$ are shown in figure 6. Also shown for comparison are a calculated point for $k = 0$ (from method of ref. 2) which indicated good agreement and the measured yawing moments and corresponding phase angles for a plan form similar to the fin alone and for the same plan form with a tip tank attached in the manner of a pylon-mounted external store (averaged from ref. 3). The yaw axis of the model used in the present investigation corresponds to the pitch axis of the model used in reference 3, rotated 90° with respect to the horizon. It may be seen from figure 6 that the yawing moment for the T-tail configuration has approximately the same magnitude as the moment on the similar plan form with the plain tip tank (no fins), whereas it is much higher than the yawing moment for the plan form similar to the fin alone. The higher value would be expected for the T-tail since the horizontal stabilizer could be considered as an end plate. The phase angles for all three configurations decrease with increasing reduced-frequency parameter with the T-tail indicating the greatest decrease. All phase angles indicate a stable yawing moment throughout the range of k shown. It may, therefore, be concluded that the overall yawing moment on the T-tail configuration becomes more stable and increases in magnitude with increasing reduced-frequency parameter.

Side Force

The vertical-surface side-force coefficients and phase angles are shown in figure 7. Again, for comparison, are shown a calculated point for $k = 0$ (by method of ref. 2) which indicated good agreement and measured coefficients for a plan form similar to the rudder with and without a tip tank (ref. 3). The phase angles for the T-tail configuration follow a trend with reduced-frequency parameter similar to that of the measured phase angles of reference 3. The magnitude of the phase angle for the T-tail is smaller than for the similar plan form throughout the range of k shown. The phase angle increases with increasing reduced-frequency parameter. The side-force coefficients on the T-tail, which were essentially constant, also follow the same trend as the coefficients for the similar plan form with and without the tip tank. It may be noted that the use of the tip tank increases the magnitude of the side-force coefficients for the fin alone and that the addition of the horizontal stabilizer increases the magnitude of the coefficient slightly more than the addition of the tip tank. This increase would be expected because of the end-plate effect of the horizontal stabilizer.

CONCLUSIONS

Some aerodynamic forces and moments associated with the yawing oscillations of a T-tail configuration have been given as well as the horizontal-stabilizer rolling-moment coefficients about an axis at the tip of the vertical fin. Comparisons of total yawing-moment and side-force coefficients and the corresponding phase angles have been made with those of a similar plan form with and without a plain tip tank attached. Some calculated results for a reduced-frequency parameter k of zero are included. From the results given, the following conclusions are made:

1. The horizontal-stabilizer rolling-moment coefficients decreased with increasing reduced-frequency parameter. The corresponding phase angles showed a general trend of increasing. The calculated coefficients from the results of previous work for the steady case ($k = 0$) indicated a smaller magnitude than would be obtained from an extrapolation of the experimental coefficients.
2. The total rolling-moment coefficient decreased only slightly with increasing reduced-frequency parameter, whereas the corresponding phase angles increased. The calculated coefficient for $k = 0$ was in good agreement.
3. The total yawing-moment coefficients increased with increasing reduced-frequency parameter and the corresponding phase angles decreased.

The calculated coefficient at $k = 0$ indicated good agreement. The coefficients for the present T-tail configuration are greater than those for a plan form similar to the T-tail fin.

4. The vertical-surface side-force coefficients were essentially constant with increasing reduced-frequency parameter, whereas the corresponding phase angles increase. The calculated coefficient at $k = 0$ was in good agreement. The coefficients for the present T-tail configuration are greater than those for a plan form similar to the T-tail fin.

Langley Aeronautical Laboratory,
National Advisory Committee for Aeronautics,
Langley Field, Va., July 25, 1958.

REFERENCES

1. Mangler, W.: The Lift Distribution of Wings With End Plates. NACA TM 856, 1938.
2. Queijo, M. J., and Riley, Donald R.: Calculated Subsonic Span Loads and Resulting Stability Derivatives of Unswept and 45° Sweptback Tail Surfaces in Sideslip and in Steady Roll. NACA TN 3245, 1954.
3. Clevenson, Sherman A., and Leadbetter, Sumner A.: Some Measurements of Aerodynamic Forces and Moments at Subsonic Speeds on a Wing-Tank Configuration Oscillating in Pitch About the Wing Midchord. NACA TN 3822, 1956.
4. Clevenson, Sherman A., and Widmayer, Edward, Jr.: Experimental Measurements of Forces and Moments on a Two-Dimensional Oscillating Wing at Subsonic Speeds. NACA TN 3686, 1956. (Supersedes NACA RM L9K28a.)

TABLE I

RESULTS OF AN EXPERIMENTAL INVESTIGATION ON A T-TAIL CONFIGURATION

| k | q , lb/sq ft | $ C_Y, \psi $ | $\phi_{Y, \psi}$, deg | $ C_l, \psi $ | ϕ_l, ψ , deg | $ C_l, \psi $ | ϕ_l, ψ , deg | $ C_n, \psi $ | ϕ_n, ψ , deg |
|-------|-------------------|---------------|---------------------------|---------------|-------------------------|---------------|-------------------------|---------------|-------------------------|
| 0.090 | 260 | 1.247 | -1 | 0.256 | -4 | 2.56 | -1 | 0.602 | -2 |
| .092 | 247 | 1.203 | -1 | .236 | -3 | 2.48 | -1 | .613 | -6 |
| .0955 | 234 | 1.222 | -1 | .234 | -4 | 2.38 | -1 | .608 | -6 |
| .105 | 209 | 1.306 | -1 | .264 | -4 | 2.74 | -1 | .616 | -8 |
| .115 | 184 | 1.242 | 0 | .250 | -4 | 2.62 | 0 | .650 | -7 |
| .116 | 182 | 1.194 | 0 | .231 | -4 | 2.48 | -1 | .653 | -2 |
| .128 | 162 | 1.213 | 0 | .222 | -4 | 2.52 | 0 | .599 | -11 |
| .142 | 138 | 1.101 | 0 | .199 | -4 | 2.30 | 0 | .656 | -10 |
| a.156 | 287 | 1.39 | 0 | .262 | -4 | (b) | (b) | .680 | -13 |
| .158 | 118 | 1.132 | 0 | .226 | -4 | 2.38 | 0 | .636 | -12 |
| .160 | 116 | 1.086 | 0 | .212 | -4 | 2.30 | 0 | .628 | -13 |
| .182 | 94 | 1.188 | 0 | .216 | -5 | 2.40 | 1 | .648 | -14 |
| a.194 | 230 | 1.36 | 1 | .224 | -4 | (b) | (b) | .662 | -17 |
| a.195 | 228 | 1.40 | 1 | .234 | -4 | (b) | (b) | .668 | -17 |
| .202 | 79 | 1.215 | 0 | .204 | -5 | 2.30 | 1 | .671 | -17 |
| .204 | 79 | 1.190 | 0 | .198 | 0 | 2.22 | 0 | .755 | -15 |
| .216 | 70 | 1.120 | 0 | .199 | -5 | 2.24 | 2 | .722 | -18 |
| .240 | 59 | 1.228 | 2 | .196 | -4 | 2.30 | 3 | .730 | -21 |
| a.240 | 174 | 1.31 | 3 | .210 | -3 | (b) | (b) | .691 | -20 |
| .280 | 44 | 1.140 | 3 | .177 | -2 | 2.32 | 4 | .806 | -27 |
| a.291 | 131 | 1.39 | 6 | .199 | -3 | (b) | (b) | .757 | -26 |
| .298 | 39 | 1.167 | 4 | (b) | (b) | 2.38 | 6 | .827 | -27 |
| .331 | 32 | 1.197 | 6 | (b) | (b) | 2.36 | 8 | .954 | -29 |
| a.353 | 102 | 1.23 | 9 | .170 | -1 | (b) | (b) | .748 | -39 |
| .387 | 24 | 1.137 | 9 | (b) | (b) | 2.18 | 10 | 1.072 | -27 |
| a.435 | 70 | 1.23 | 15 | .137 | 4 | (b) | (b) | .901 | -70 |
| a.557 | 47 | 1.10 | 22 | .123 | 9 | (b) | (b) | .945 | -70 |

^aData obtained in Freon.^bData not obtained.

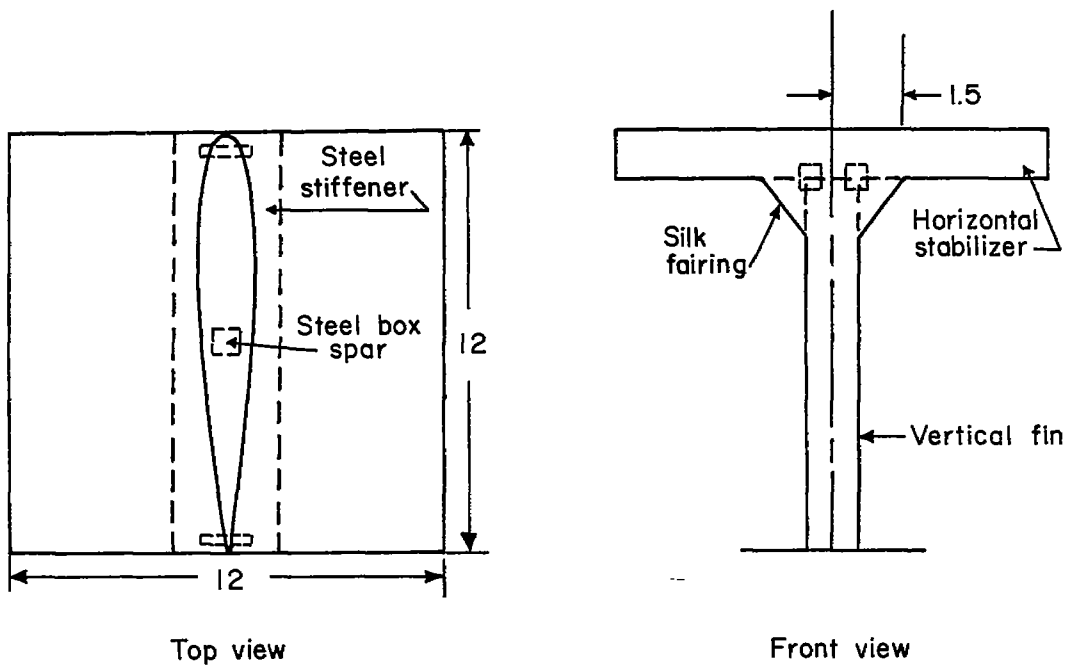


Figure 1.- Schematic diagram of T-tail configuration. All dimensions are in inches.

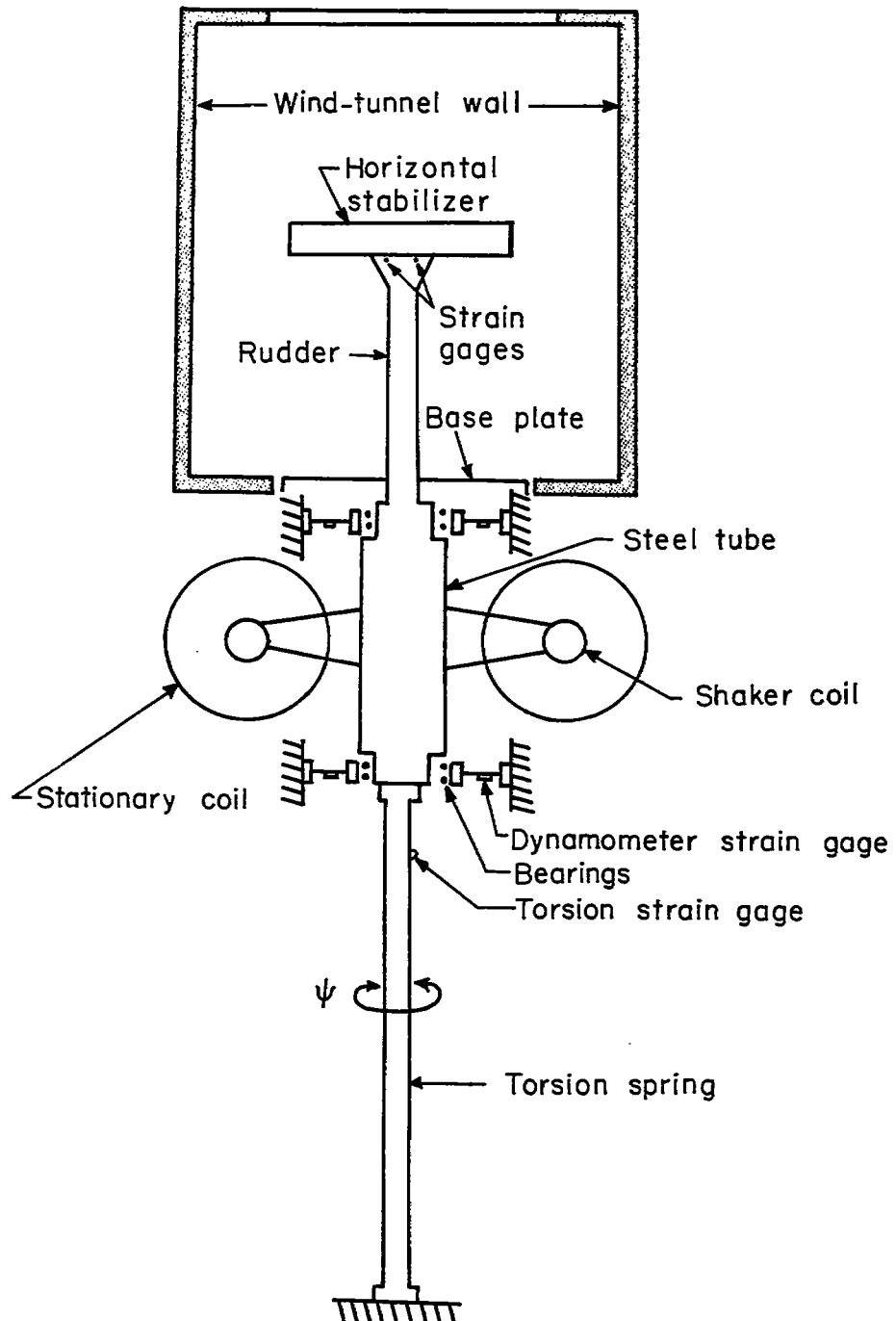


Figure 2.- Diagrammatic view of oscillator mechanism and T-tail combination mounted in the Langley 2-foot transonic flutter tunnel.

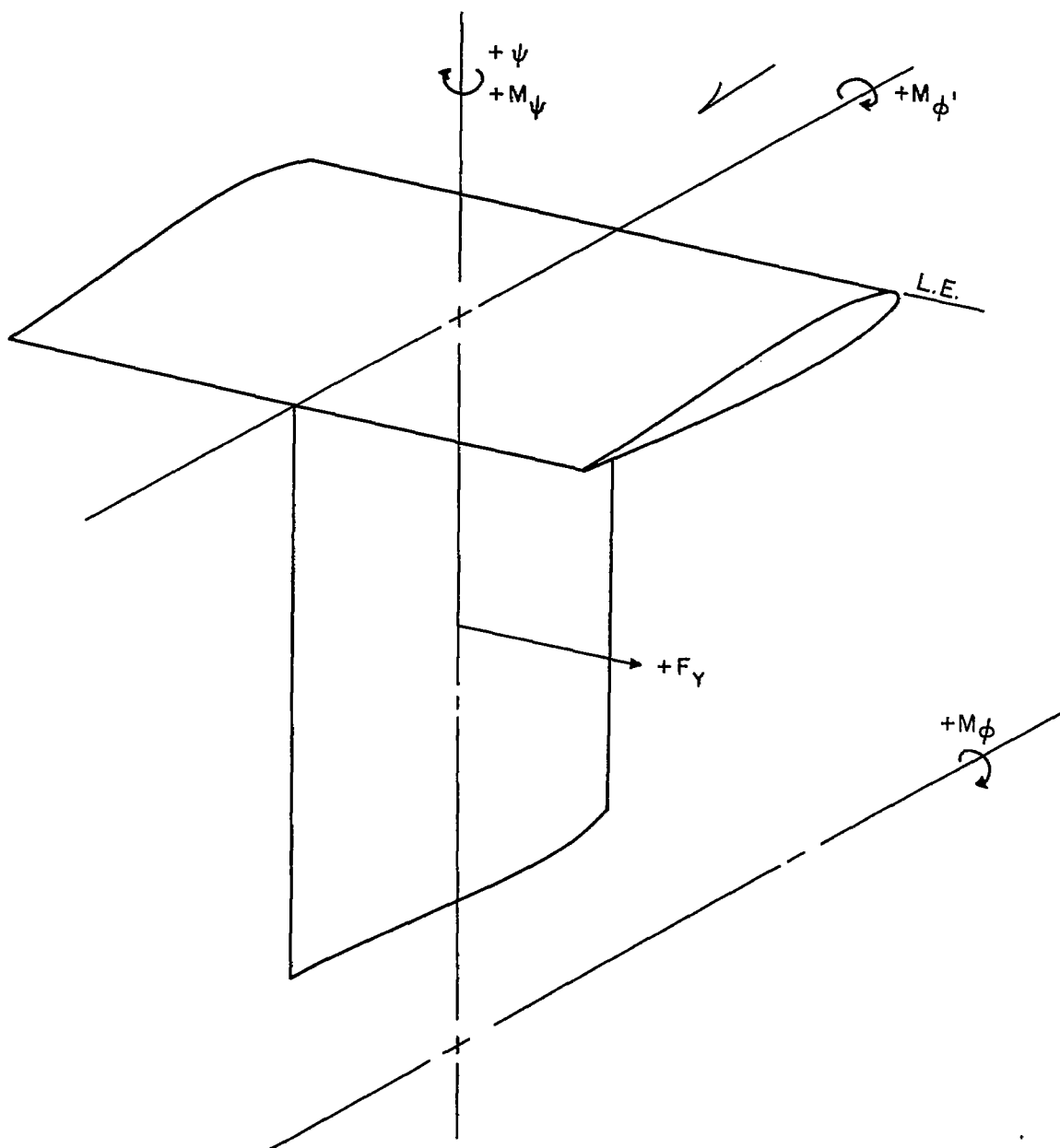


Figure 3.- Schematic diagram of T-tail configuration indicating sign convention.

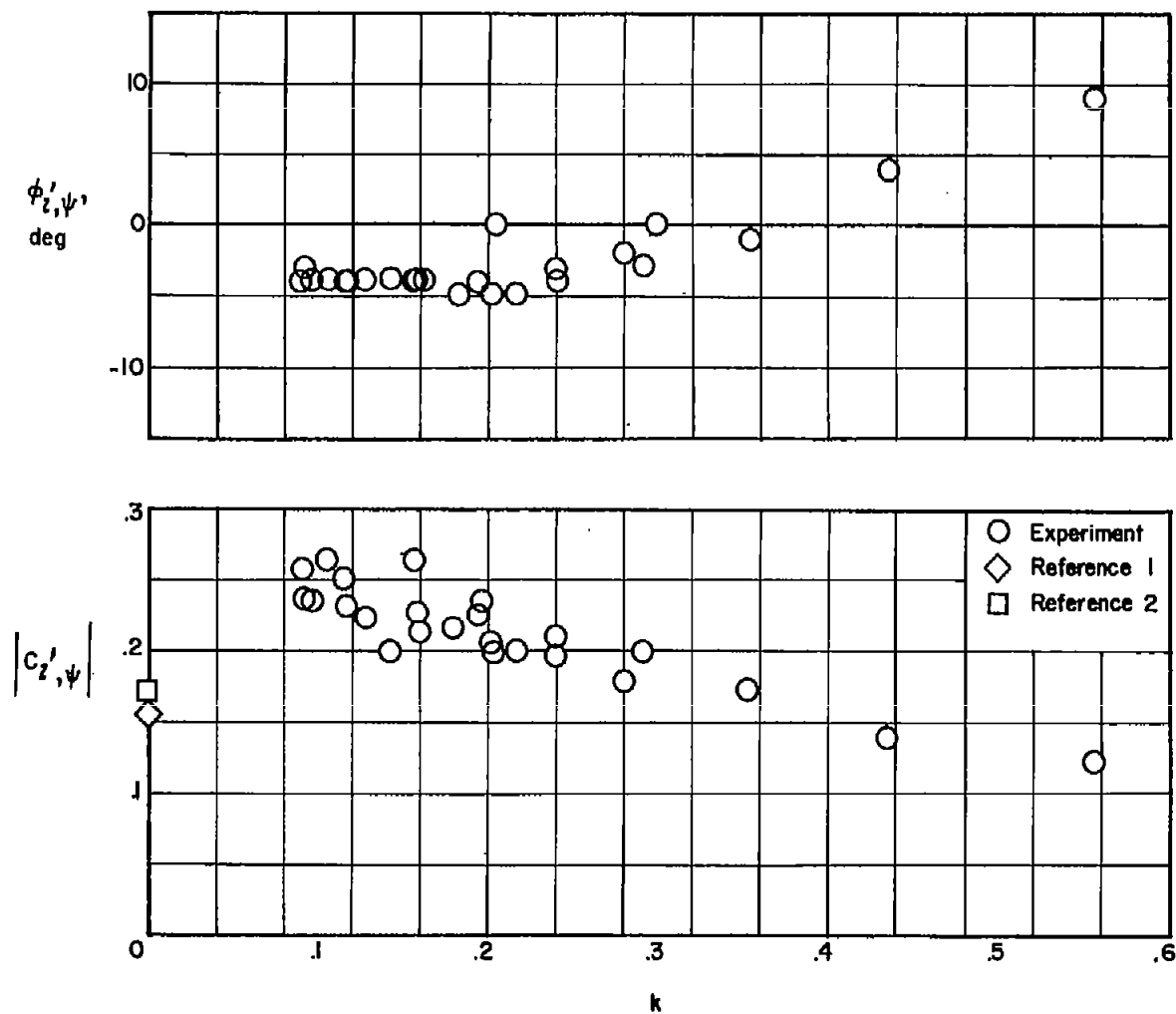


Figure 4.- Variation of the horizontal-stabilizer rolling-moment coefficient and phase angle with reduced-frequency parameter. Values for $k = 0$ are calculated by methods of references 1 and 2.

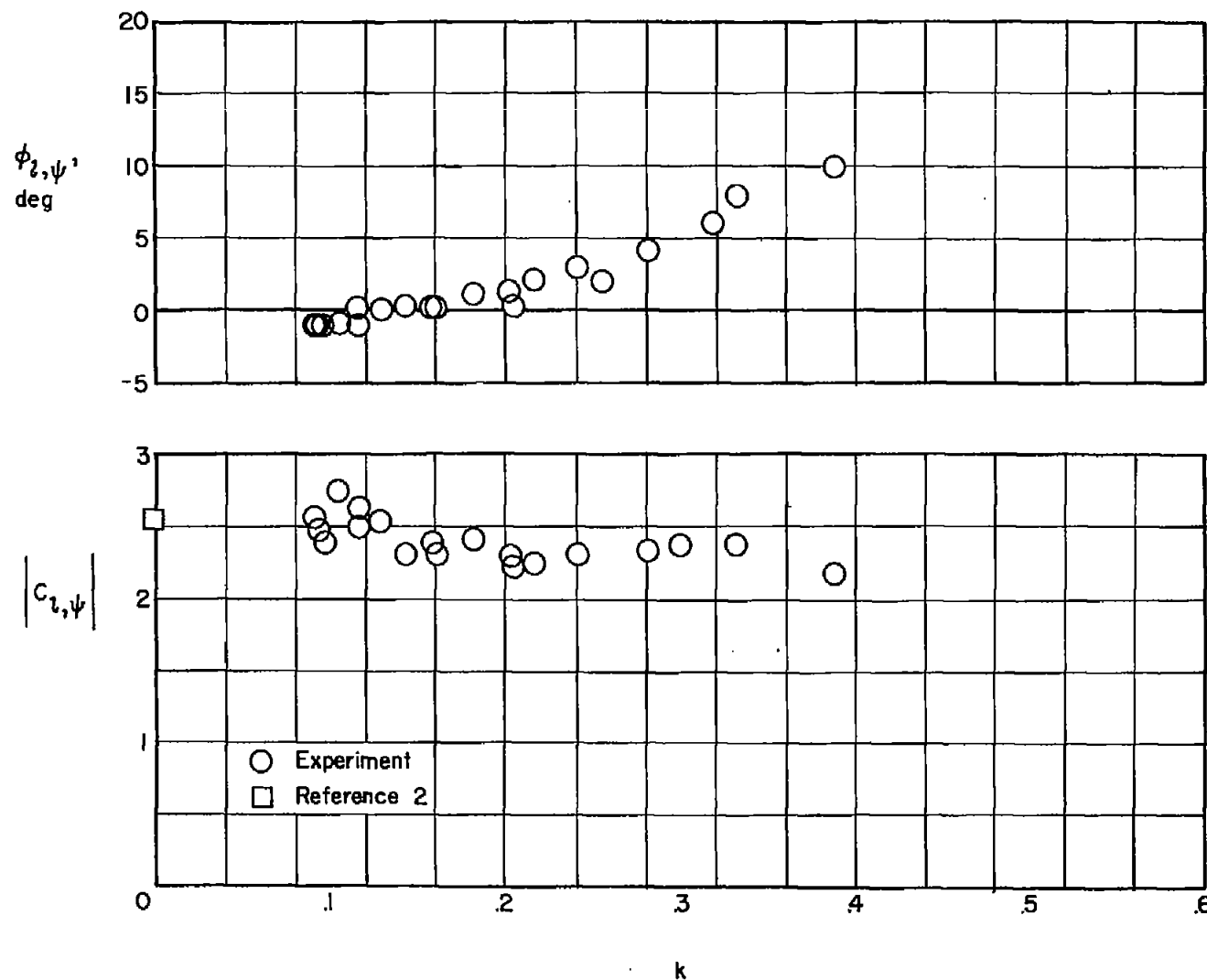


Figure 5.- Variation of the total rolling-moment coefficient and phase angle with reduced-frequency parameter.

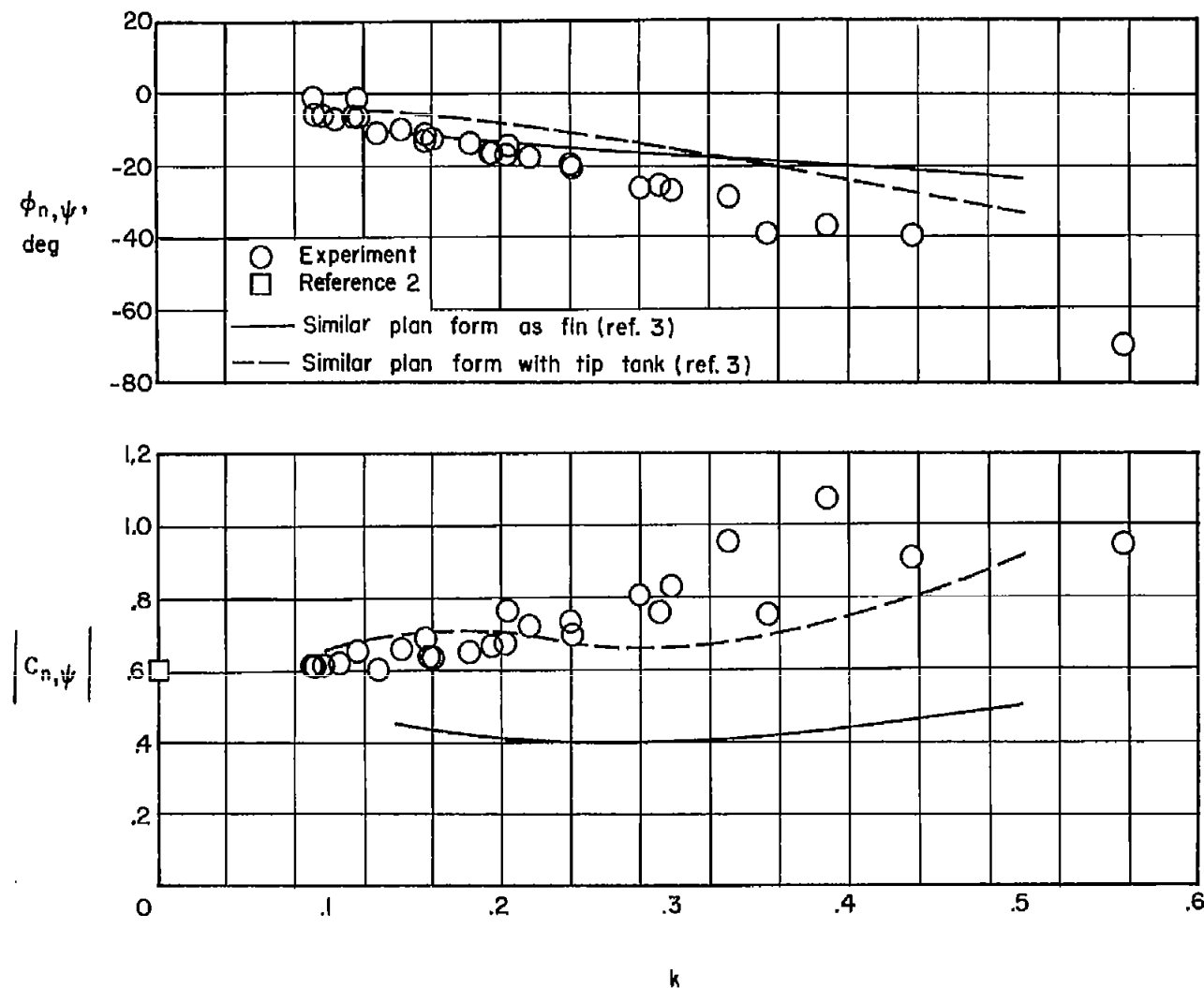


Figure 6.- Variation of the total yawing-moment coefficient and phase angle with reduced-frequency parameter.

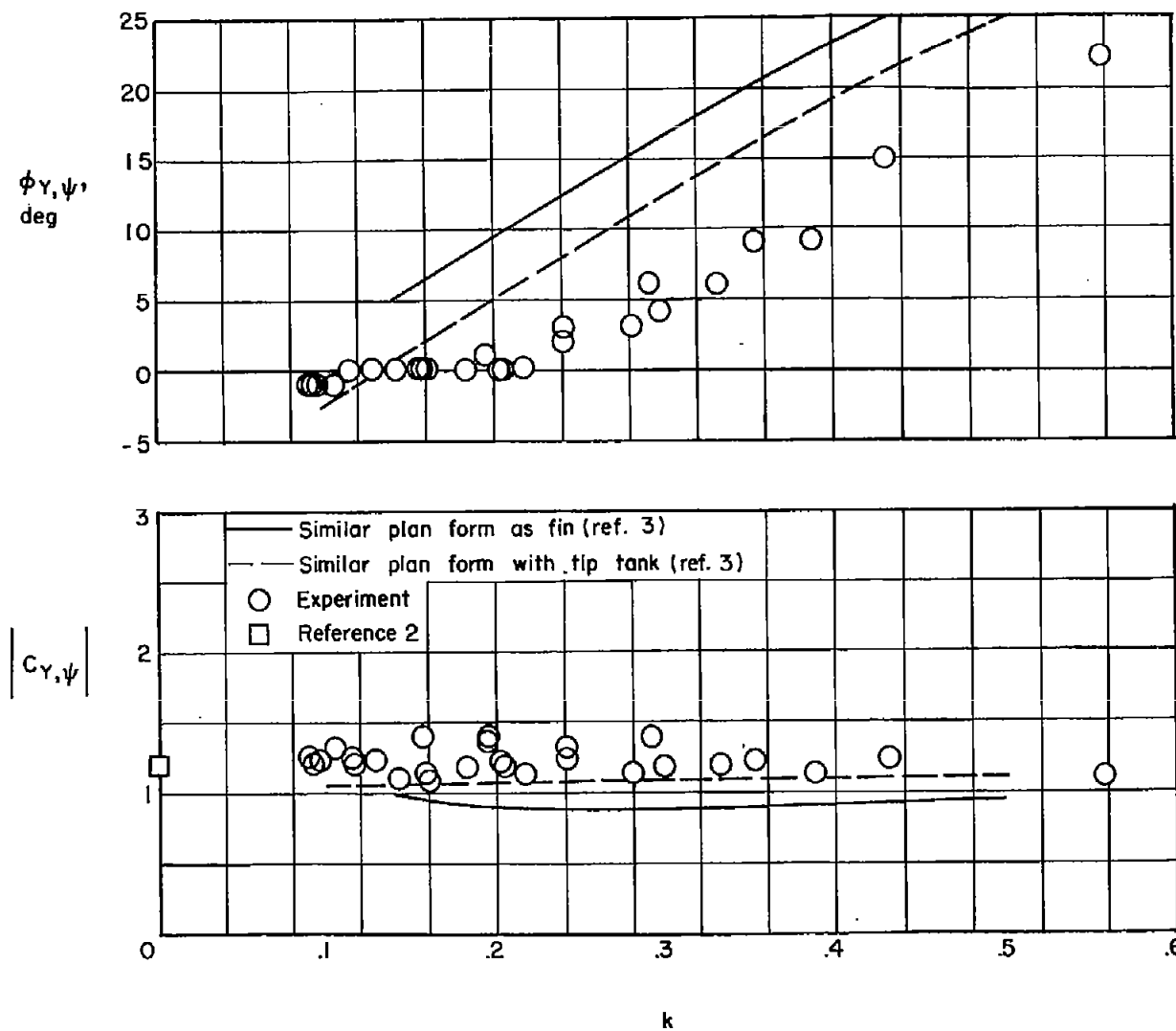


Figure 7.- Variation of the vertical-surface side-force coefficient and phase angle with reduced-frequency parameter.